



Reprinted from JOURNAL OF THE ELECTROCHEMICAL SOCIETY  
Vol. 132, No. 3, March 1985  
Printed in U.S.A.  
Copyright 1985

## Semiconductor Electrodes

### LVI. Principles of Multijunction Electrodes and Photoelectrosynthesis at Texas Instruments' p/n-Si Solar Arrays

James R. White, Fu-Ren F. Fan, and Allen J. Bard\*

*Department of Chemistry, The University of Texas Austin, Texas 78712*

#### ABSTRACT

In photoelectrochemical (PEC) cells based on single junctions of semiconductors with solutions or metals, photopotentials are rarely above 0.6-0.8V. The higher photovoltages needed to drive more energetic reactions require multijunction cells involving multilayer electrodes or series connection of PEC cells. Such PEC cells are considered, and their behavior is shown to be predicted from the current-potential (i-V) behavior at each interface; the sum of the voltage drops at a given current yields the i-V characteristic of the overall PEC cell. These principles are illustrated with the Texas Instruments arrays based on silicon spheres and Si p/n junctions contacting a solution via a noble metal layer. Reactions considered include generation of  $\text{Cl}_2$  with reduction of  $\text{O}_2$  or the generation of  $\text{H}_2$ , the photobromination of phenol, and the photochlorination of cyclohexene in acetonitrile.

Liquid-junction photoelectrochemical (PEC) cells are of interest in the direct utilization of solar energy to carry out useful chemical reactions (1-4). In most liquid-junction PEC cells, the photopotential arises at the semiconductor/solution interface. The maximum (open-circuit) photopotential, which represents the driving force of the cell chemical reaction, is rarely more than 0.8V, and is often below 0.6V. This rather low driving force limits the

range of possible photoelectrosynthetic reactions which can be carried out in PEC cells without the application of an external bias. Alternatively, the photoactive junction can be at a metal/semiconductor (Schottky barrier) interface with the faradaic reaction occurring at the metal (sometimes bearing an appropriate electrocatalyst). For example, PEC's with the following junctions have been described: Au/n-GaP (5, 6), PtSi/n-Si (7), and Pt/n-GaAs (8). Such cells have the advantage that the semiconductor is protected from the solution environment and show

\* Electrochemical Society Active Member.

photopotentials that are independent of the redox potential of solution species. However, again the reported photopotentials are usually below 0.6V. Related PEC's involve photopotentials that arise at a p/n semiconductor junction, again protected from the solution by a metal overlayer. The most highly developed systems of this type are probably the p-Si/n-Si junctions separated from the solution by suitable noble metal overlayers that are used in the Texas Instruments Solar Energy System (TISES) (9-11). The photopotential developed at these junctions is about 0.55V. These latter p-Si/n-Si junctions are clearly related to solid-state photovoltaic cells (e.g., involving single-crystal Si) that are used for electricity production. In the TISES system, these junctions are produced on small (0.2 mm diam) Si spheres that are embedded in glass and backed by a conductive matrix to form arrays in contact with a solution. The relative advantages of these arrays compared to solid-state devices has been discussed (10, 11).

If more energetic reactions are to be driven in PEC cells without an external bias, cells with both photoactive anodes and cathodes can be employed. These two electrodes must be matched carefully to maximize the efficiency, since two photons are used to drive a single electron through the circuit. This strategy is employed in the TISES system, where both n-Si on p-Si spheres (photocathodes) and p-Si on n-Si spheres (photoanodes) are coupled to produce a total open-circuit voltage of 1.1V. These microspheres are coated with noble metal films which act as electrolytic contacts to the solution, stabilize the substrate Si, and catalyze the electrode reactions. The TISES system has been developed specifically for the overall conversion of solar to electrical energy in a system where HBr is decomposed by sunlight to form Br<sub>2</sub> at the photoanode and H<sub>2</sub> at the photocathode. The Br<sub>2</sub> and H<sub>2</sub> are stored and subsequently recombined in a fuel cell to produce electricity.

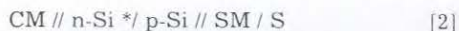
To form systems with higher output voltages, a number of junctions must be connected in series or the PEC cells must be coupled in a suitable way. Particularly interesting structures would involve multilayer devices with several photoactive junctions, especially if semiconductors with different bandgaps are employed. Structures of this type have been proposed in solid-state photovoltaic devices (tandem or cascade cells) (12), but few examples have been given in photoelectrochemical cells for direct utilization of radiant energy in chemical reactions. In this paper, we consider the principles of semiconductor electrode devices with interior photoactive junctions and the means of coupling PEC cells to increase the available voltage to levels consistent with a particular reaction. In particular, we demonstrate the application of the Texas Instruments solar arrays to electrosynthetic reactions, e.g., in the production of chlorine and oxygen and in the bromination of phenol. The utilization of these arrays in a nonaqueous solvent (MeCN) for the chlorination of cyclohexene is also described.

### Principles of Operation

We suggest the following notation for multilayer semiconductor devices



where CM represents the contact metal to the electrode (connected to an external lead), A and B represent other, often semiconductor phases, SM is the surface metal or layer contacting the solution phase, and S is the solution. As usual in electrochemical cells, a slash represents a junction; we represent an ohmic contact by //. For example, the Texas Instruments photoanode (TIA), which is part of the array used in this work, is represented as



where CM is the tantalum back contact, and SM is a surface metal (e.g., Pt or Ir) with a suitable catalyst. The photoactive junction (indicated by the asterisk) is the Si

n/p junction. This can also be denoted as an L<sub>4</sub>P<sub>1</sub> electrode, where L represents the number of layers used and P the number of photoactive junctions. The TI photocathode (TIC) is thus



and the array is formed by contacting CM and CM'.

The operation and current-voltage (i-V) curves of a given electrode can be understood by examining the i-V characteristics of each junction and noting that these are connected in series. Operation of the total cell can then be obtained, as is usual for electrochemical devices, by combining the i-V characteristics of each electrode. Consider the TIA shown in Eq. [2]. The electrochemical behavior is described by that of the p/n junction, either in the dark or under irradiation, in series with the SM/S interface (Fig. 1). For the p/n junction the dark behavior (curve A) is given by the Shockley Eq. [4] (13)

$$j = j_s [ \exp (eV_j/kT) - 1 ] \quad [4]$$

where  $j$  is the current density,  $j_s$  is the saturation current density for the junction as determined by the carrier density, mobility, and diffusion length, and  $V_j$  is the voltage drop across this junction. The illuminated p/n junction (curve B) behaves as a constant current source in parallel with the junction and the  $j$ - $V$  relationship is given by

$$j = j_s [ \exp (eV_j/kT) - 1 ] - j_i \quad [5]$$

where  $j_i$  is the constant current produced by photogeneration of carriers in the junction. The metal/solution junction shows behavior that depends upon the nature of the metal and solution components and is governed by the typical electrochemical thermodynamic, mass-transport, and kinetic considerations (14). A representative curve is given in Fig. 1C, showing the current across this junction as a function of the potential of SM vs. a reference electrode,  $V_{SM}$ . The  $j$ - $V$  behavior of the multilayer structure is given by the summation of the  $j$ - $V_j$  and  $j$ - $V_{SM}$  curves, assuming a series connection (Fig. 1D). At any current density,  $j$ , the voltage drop between CM and the reference electrode,  $V$ , is  $V_j + V_{SM}$  (plus any  $iR$  drops within the phases). Clearly, the light driven photopotential (or the underpotential for the electrode reaction because of the p/n junction), at any value of  $j$ , is  $V_j$ . The behavior of the TIC shown in Eq. [3] can be obtained in an analogous manner, as shown in Fig. 2. The characteristics of multilayer, multijunction devices, e.g., containing several photoactive junctions, can be obtained in a similar way by adding the  $j$ - $V$  characteristics of each junction.

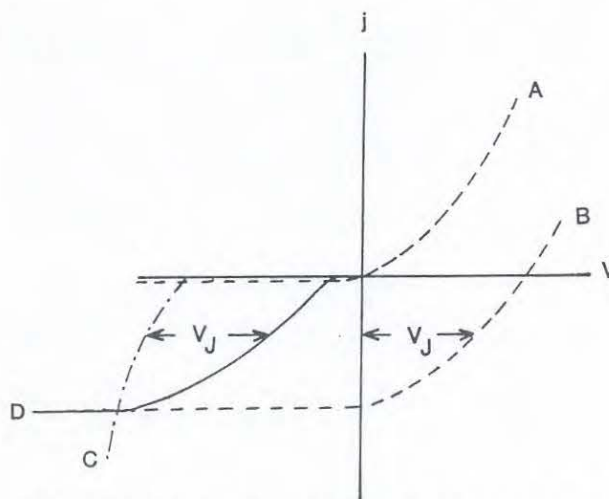


Fig. 1. Representative  $j$ - $V$  curves for p on n-Si junction in the dark (A) and in the light (B). Voltage scale for curves A and B represents a voltage drop, ( $\Delta V = V_j$ ) across the p/n junction. (C):  $j$ - $V$  curve for a metal/solution junction. (D);  $j$ - $V$  curve for total TIA. Potentials are vs. a reference electrode.

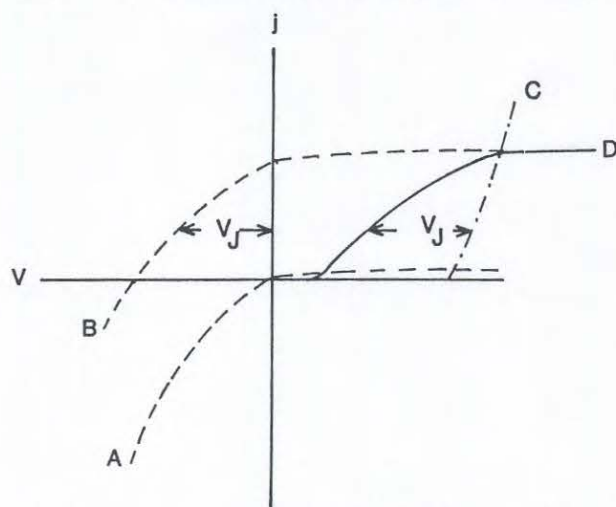


Fig. 2. Representative  $j$ - $V$  curves for n on p-Si junction in the dark (A) and in the light (B). Voltage scale for A and B represents a voltage drop,  $\Delta V = V_J$ , across the n/p junction. (C):  $j$ - $V$  curves for a metal electrode; (D):  $j$ - $V$  curve for total TIC. Potentials are vs. a reference electrode.

**Single photoelectrode cells.**—The behavior of the overall photoelectrosynthetic cell, e.g., TIA/S/M, where M is the conductive counterelectrode, is determined by the  $i$ - $V$  curve of the TIA discussed above, the  $i$ - $V$  curve of electrode M (in the cathodic region) and any  $iR$  drop in solution, under the conditions that the total anodic current at the TIA is equal to the cathodic current at M at any given cell voltage,  $V_{\text{cell}}$ . Representative curves are given in Fig. 3. The maximum current in the absence of any externally applied voltage would be  $i_{\text{sc}}$ , the short-circuit current. Clearly, for a spontaneous reaction, good overlap of the anodic and cathodic  $i$ - $V$  curves is required. The  $i$ - $V$  curve for a variable load resistor,  $R_L$ , across the cell, represented by  $V_{\text{cell}}$ , or with an externally applied voltage,  $V_{\text{appl}}$ , can also be obtained (Fig. 3). The maximum photocurrent under any conditions [in the absence of current doubling effect (15)] is  $i_L$ , governed by the p/n junction characteristics. An analogous treatment applies for the TIC coupled in a cell with a metal anode.

**Systems with two photoelectrode (dual-array PEC).**—When one photoelectrode is coupled with a metal counterelectrode, the maximum open-circuit photovoltage,  $V_{\text{oc}}$ , is limited by the potential generated at a single p/n junction, e.g., for a silicon p/n junction, 0.55V. However, if a photoanode is coupled with a photocathode,  $V_{\text{oc}}$  is the sum of both photoactive junction potentials. Thus, for the cell TIC/S/TIA,  $V_{\text{oc}} = 1.1\text{V}$ . This allows more energetic reactions to be driven without an external bias. Again, the overall cell behavior can be predicted from the individual  $i$ - $V$  curves for the TIA and TIC. This is shown in Fig. 4.

**Multiple photoarray system.**—To obtain even higher potentials to drive more energetic reactions, two (or more) photocells must be coupled. For example, by suitable coupling of the photocells: TIC/S/TIA and TIC/S'/TIA an open-circuit photovoltage of 2.2V can be obtained across solution S'. In this case, cell 1 would contain a single redox couple (e.g.,  $\text{Br}_2/\text{Br}^-$ ) and behaves as a photovoltaic cell which provides a bias to cell 2 and adds to the photovoltage developed in cell 2. The mode of connection of these cells and the relevant  $i$ - $V$  curves are shown in Fig. 5, where a reaction involving  $> 1.1\text{V}$  (e.g.,  $2\text{HCl} \rightarrow \text{H}_2 + \text{Cl}_2$ ) is carried out.

The experimental results that follow illustrate  $i$ - $V$  curves for several redox couples at TI silicon arrays (TIA, TIC) and demonstrate several photoelectrosynthetic PEC's of the type outlined above.

### Experimental

The multilayered semiconductor electrodes used in these experiments were the TISES silicon arrays pro-

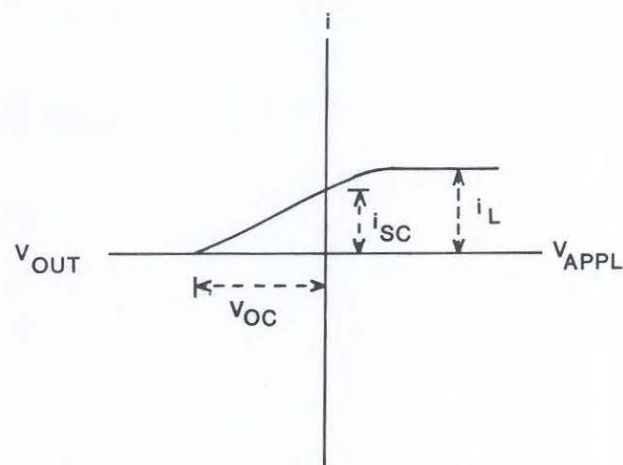
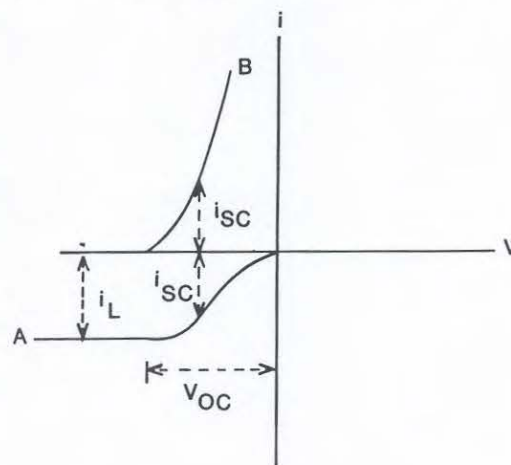


Fig. 3. Representative  $i$ - $V$  curves for the cell TIA/S/M. Top: curves A and B represent TIA and M, respectively. Potentials are vs. a reference electrode. Bottom:  $i$ - $V_{\text{cell}}$  behavior when electrodes are coupled through a load resistance,  $R_L$ . For  $R_L = 0$ ,  $i = i_{\text{sc}}$ , and  $V = 0$ ; for  $R \rightarrow \infty$ ,  $i = 0$ , and  $V = V_{\text{oc}}$ .  $V_{\text{out}}$  represents a voltage produced by the cell under illumination.  $V_{\text{appl}}$  represents a voltage applied to the cell.

duced by Texas Instruments. Electrodes were made by contacting a copper wire to the conductive back surface of the panel arrays with conductive silver paint. The con-

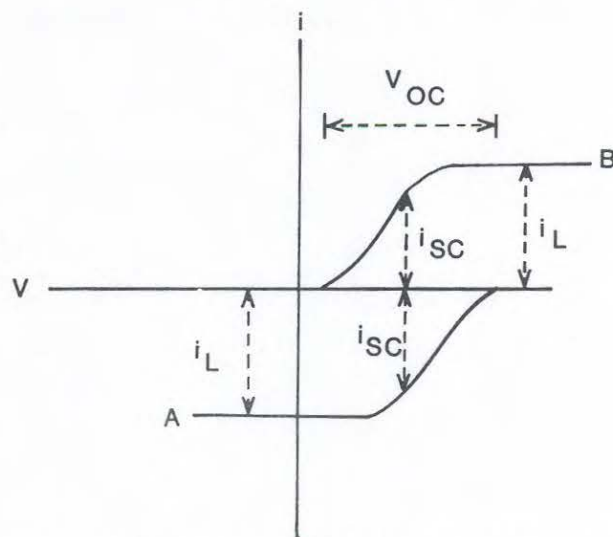


Fig. 4. Representative  $i$ - $V$  curves for the cell TIA/M/TIC. Potentials are vs. a reference electrode. Curves A and B represent TIA and TIC, respectively.

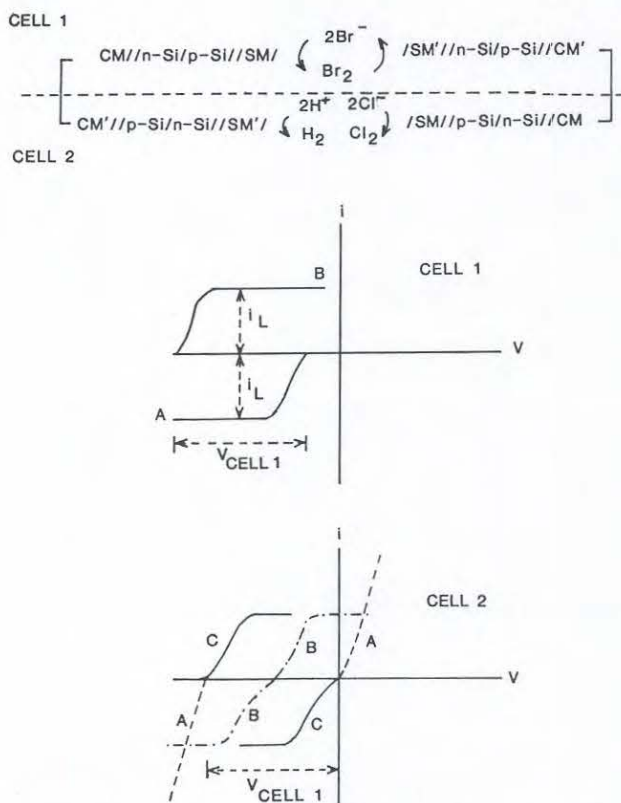


Fig. 5. Schematic representation of dual cell photoarray system. Top: *i-V* curves for cell 1; (A) TIA, (B) TIC. Bottom: *i-V* curves for cell 2. (A) (---): Pt electrode in HCl. (B) (-.-.-): TIA and TIC in HCl under illumination. (C) (—): as in B, under bias from cell 1.

tact was covered with epoxy cement which was insulated from solution with silicone rubber. The exposed front surface geometrical area was  $0.25 \text{ cm}^2$ .  $\text{RuO}_2$  films were prepared by decomposition of  $\text{RuO}_4$  vapor, which was prepared chemically (16), onto ambient temperature substrates. XPS data showed that the binding energies for the Ru  $3d_{5/2}$  line from samples prepared in this manner are in agreement with those obtained for anhydrous  $\text{RuO}_2$  powder (17).

Voltammetric experiments were performed in a single-compartment Pyrex cell with a volume of 50 ml. All solutions were degassed with prepurified  $\text{N}_2$  for 15 min prior to use unless indicated otherwise. Voltammograms were recorded with a Princeton Applied Research (PAR) Model 173 potentiostat/galvanostat, a PAR Model 175 Universal Programmer, and a Houston Instruments Model 2000 X-Y Recorder. The illumination source was a tungsten-halogen lamp with a 13 cm water filter.

A dual-compartment Plexiglas cell (40 ml each compartment) was used for experiments involving multiple photoelectrodes immersed in two solutions. For the experiment involving HCl electrolysis, one compartment contained HCl while the other contained the  $\text{Br}^-/\text{Br}_2$  redox couple. Photoelectrodes were placed as close to the cell wall as possible to minimize absorption of light by the solution.

A Pyrex H-cell was used for the experiments in which  $\text{Cl}_2$  was produced by reduction of  $\text{O}_2$  (TIA/S/M). A fuel cell electrode (geometrical area,  $3.1 \text{ cm}^2$ ), Teflon/carbon/platinum (donated by TI), was used as a cell divider. One compartment contained 5M HCl, and the other was kept dry and pressurized with  $\text{O}_2$ .

Power characteristics were evaluated with a series, variable resistance box and a digital voltmeter. Short-circuit measurements were approximated by using a  $15\Omega$  resistance and measuring the corresponding voltage drop. All chemicals were reagent grade and were used without further purification. Triply distilled water was used in all

experiments. Acetonitrile was dried over molecular sieves.

## Results and Discussion

**Half-reactions at TIA's and TIC's.**—We considered half-cells composed of a TIA immersed in different solutions (cell [2]) and compared the photoresponse of these to the *i-V* curves at a metal electrode.

**Oxidation of chloride.**—The voltammetric curves for a TIA in 10.0M LiCl are shown in Fig. 6. In the dark, curve A, essentially no current is observed, even at potentials where vigorous  $\text{Cl}_2$  production is observed on a bare Pt electrode (curve C). Under illumination, at a light intensity of  $170 \text{ mW/cm}^2$ , *j-V* curve B results. The limiting current density,  $j_l$ , was  $38 \text{ mA/cm}^2$ . The open-circuit photopotential,  $V_{oc}$ , was 0.49V, as measured from the differences between curves B and C. The platinum disk electrode operated near the reversible potential for the  $\text{Cl}/\text{Cl}_2$  couple at low current densities. The fill factor was 0.42. The stability of the TIA for  $\text{Cl}_2$  evolution was tested by holding it at  $\pm 1.0\text{V}$  vs. SCE under illumination of  $170 \text{ mW/cm}^2$  for 48h; voltammograms taken intermittently during this time period showed no change in  $j_l$  or in the *j-V* curve. No apparent changes in the electrode surface were observed.

The effect of thin films of  $\text{RuO}_2$ , a known catalyst for chlorine evolution, on the voltammetric response in  $\text{Cl}^-$  media was also examined. Films about  $100\text{\AA}$  thick were deposited by chemical vapor deposition onto ambient temperature substrates. The TIA/ $\text{RuO}_2$  electrode showed a slightly more negative onset for chlorine evolution compared to an unmodified TIA (Fig. 7). The modified TIA also showed a larger cathodic peak on the reverse scan. These results suggest that the kinetics of the  $\text{Cl}^-/\text{Cl}_2$  couple are somewhat improved by the  $\text{RuO}_2$  treatment. The fill factor for the  $\text{RuO}_2$  coated anode increased to 0.48. There was, however, some attenuation of  $j_l$ , because of light absorption by the  $\text{RuO}_2$  layer (25% attenuation in the worst case). The  $\text{RuO}_2$  modified TIA's were tested for stability by potential cycling for 1h under illumination. The films showed stable operation for solutions of  $\text{pH} > 2$ ; however, for  $\text{pH} < 1$ , the *i-V* curves showed only resistive behavior with poor photoeffects, indicating deterioration of the surface film.

**The  $\text{Br}^-/\text{Br}_2$  couple.**—This couple is of interest because photogenerated  $\text{Br}_2$  could be employed in brominations of organics and because this couple could be used in a photovoltaic mode in the coupling of two PEC's. Typical *i-V* curves are shown in Fig. 8 for the TIA and TIC electrodes. The data pertaining to this couple are given in Table I.

**$\text{Fe(III)/Fe(II)}$  couples.**—We also investigated the  $\text{Fe}^{3+}/\text{Fe}^{2+}$  couple in 1M HCl medium and the  $\text{Fe}(\text{CN})_6^{3-}/\text{Fe}(\text{CN})_6^{4-}$  couple in 0.5M  $\text{Na}_2\text{SO}_4$  for use in the photovoltaic biasing cell. The

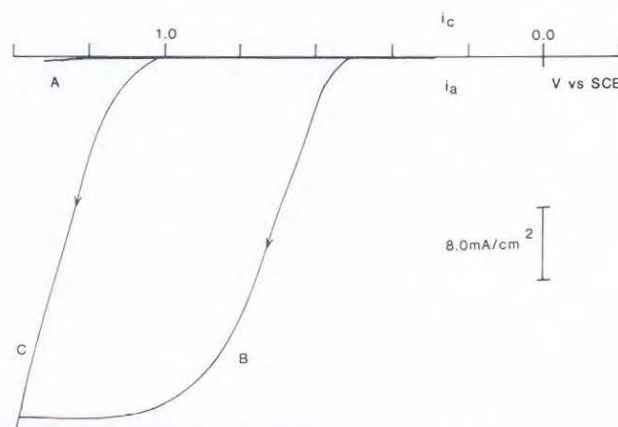


Fig. 6. *j-V* behavior for a TIA in 10M LiCl in the dark (A) and under illumination of  $170 \text{ mW/cm}^2$  (B) and for a Pt electrode (C). Scan rate:  $100 \text{ mV/s}$ .

Table I. Photovoltaic parameters of two electrode configuration (photoelectrode vs. Pt electrode)<sup>a</sup>

Electrolyte	Photoelectrode	$V_{oc}$ (V) <sup>b</sup>	$j_l = j_{sc}$ (mA/cm <sup>2</sup> ) <sup>c</sup>	f.f. <sup>d</sup>	Efficiency (%) <sup>e</sup>
0.5M Fe(CN) <sub>6</sub> <sup>4-</sup> } 0.5M Fe(CN) <sub>6</sub> <sup>3-</sup> }	anode	0.48	9	0.65	4.3
	cathode	0.45	10	0.55	3.8
2M FeCl <sub>2</sub> } 2M FeCl <sub>3</sub> } 1M HCl }	anode	0.5	13	0.6	6.0
	cathode	0.48	15	0.6	6.7
48% HBr 1M Br <sub>2</sub>	anode	0.5	23	0.5	8.8
	cathode	0.5	25	0.55	10.5

<sup>a</sup> Light intensity = 65 mW/cm<sup>2</sup>, from tungsten-halogen lamp.

<sup>b</sup> Open-circuit photovoltage.

<sup>c</sup> Short-circuit photocurrent.

<sup>d</sup> Fill factor.

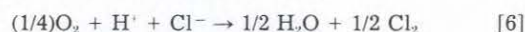
<sup>e</sup> Maximal power conversion efficiency =  $(V_{oc} \times j_{sc} \times f.f.) / \text{light intensity}$ .

results are summarized in Table I. The efficiency with these couples was lower than that found with the Br<sup>-</sup>/Br<sub>2</sub> couple. This can primarily be attributed to lower values of  $j_l$  (and, hence,  $i_{sc}$ ). For the Fe<sup>3+/2+</sup> couple, this arises because of increased light absorption by the solution, while for the Fe(CN)<sub>6</sub><sup>3-/4-</sup> couple the relatively low solubility causes  $j_l$  to be limited by mass transfer. The latter couple also suffers from some photochemical instability (18).

**The O<sub>2</sub>/OH<sup>-</sup> system.**—The *i*-V curves for the oxidation of hydroxide ion at a TIA are given in Fig. 9. For an unbuffered solution (curve A), the *i*-V is drawn out, probably because of pH changes in the vicinity of the electrode during the oxidation as well as sluggish electron-transfer rates at the metal/solution interface. Sharper *i*-V curves occur in 1M NaOH (curve B); these show some hysteresis on scan direction which, perhaps, is caused by blockage of electrode surface by oxygen bubbles. We also examined the effect of a chemically vapor deposited layer of RuO<sub>2</sub> on the TIA. While RuO<sub>2</sub> coating had only a small effect in the unbuffered solutions (pH = 8), for the 1M NaOH there was a significant improvement in behavior. The potential for the onset of photocurrent was shifted to more negative values and the current rose more steeply (*i.e.*, the fill factor improved).

**Single photoarray cells.**—Since the total driving force for a single photoarray cell is small (0.55V), only photo-

electrosynthetic reactions which have both a small positive  $\Delta G^\circ$  and good kinetics (low overpotential) are possible. An interesting reaction possibility is the photo-production of chlorine via the reaction



At pH = 0,  $\Delta G^\circ$  is 0.13 eV. This reaction can be accomplished in a cell represented as TIA/S/M, where the metal electrode, M, is a large area (geometric, 3.1 cm<sup>2</sup>) fuel cell cathode (Pt-C-Teflon) with the *i*-V characteristics shown in Fig. 10A; this showed a 0.7V overpotential for O<sub>2</sub> reduction. The TIA *i*-V response, Fig. 12A, shows poor overlap with that of M; thus, large photocurrents would not be expected upon coupling the two electrodes. Experimentally,  $i_{sc}$  was 0.5 mA/cm<sup>2</sup> and  $V_{oc}$  was 0.15V; these are comparatively low values, in agreement with the prediction based upon individual *i*-V characteristics. While the TIA demonstrated characteristic behavior for photo-oxidation of Cl<sup>-</sup>,

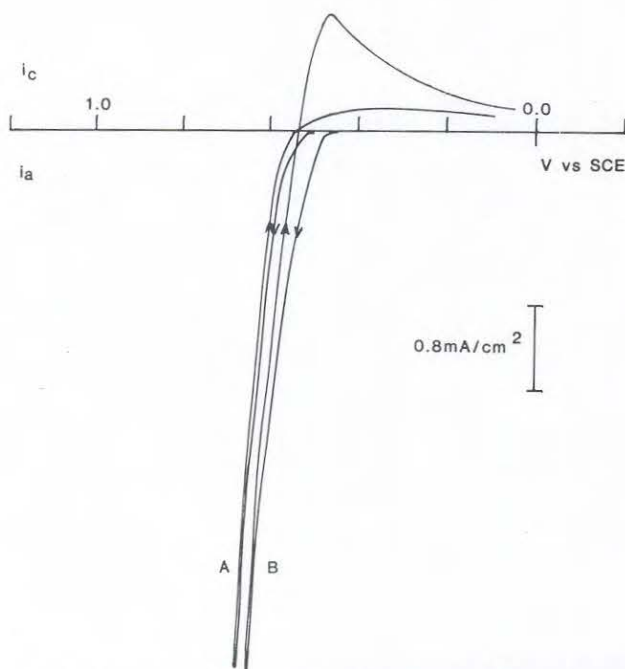


Fig. 7. *j*-V behavior for a TIA (A) and a RuO<sub>2</sub>-modified TIA (B) in 10M LiCl. Light intensity: 170 mW/cm<sup>2</sup>. Scan rate: 100 mV/s.

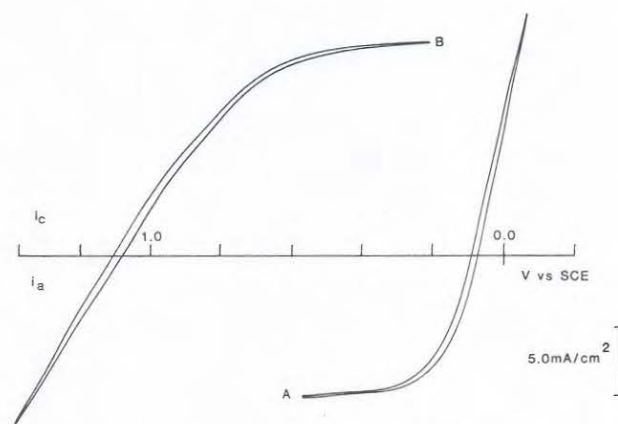


Fig. 8. *j*-V behavior for a TIA (A), TIC (B) in 48% HBr, 1.0M Br<sub>2</sub>. 170 mW/cm<sup>2</sup> light intensity. Scan rate: 100 mV/s.

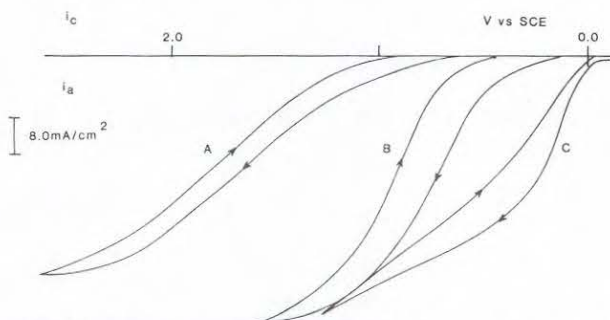


Fig. 9. *j*-V behavior for a TIA in 0.1M Na<sub>2</sub>SO<sub>4</sub> (pH = 8) (A) and in 1M NaOH (B). (C): RuO<sub>2</sub>-modified TIA in 1M NaOH. Light intensity: 170 mW/cm<sup>2</sup>. Scan rate: 100 mV/s.

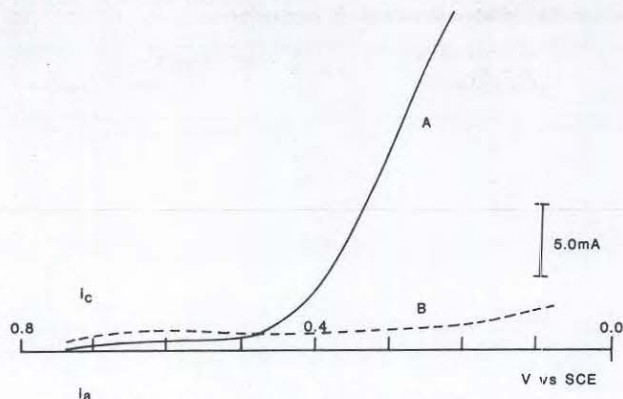


Fig. 10. *i*-*V* behavior for a fuel cell cathode (Pt-C-Teflon) with  $N_2$  flow (B) and  $O_2$  (A) in 5M HCl. Scan rate: 5 mV/s.

the cell was limited primarily because of poor kinetics for  $O_2$  reduction at the metal cathode.

**Dual photoarray cells.**—The coupling of two photoarrays, TIA/S/TIC, allows the generation of ca. 1.1V driving force for synthetic reactions. An example of a reaction in this type of cell is the bromination of phenol (18) at a TIA, coupled with the reduction of  $H^+$  at a TIC. The photo-oxidation of  $Br^-$  in 48% HBr, has a  $V_{onset}$  shifted ca. 0.55V more negative compared to a Pt electrode (Fig. 11). On the reverse scan, a cathodic peak was observed, indicating at least some of the  $Br_2$  being produced was reduced. Addition of 1M phenol to the cell suppressed the cathodic wave and shifted  $V_{onset}$  about 50 mV more negative (curve C). The cathodic wave was absent even at scan rates of 10 V/s, indicating that the bromination of phenol is an efficient approach to preventing back electron transfer. Experiments performed with only phenol and supporting electrolyte showed no photoanodic current, indicating that the observed behavior was not due to direct oxidation of phenol.  $i_p$  for the TIA was attenuated by 20% in the presence of phenol; however, reduction of  $H^+$  at a TIC, curve D, was unchanged by phenol addition. The two photoelectrodes when coupled give a  $V_{oc}$  of 0.42V with  $i_{sc}$  of 4.5 mA.

**Multiple photoarray cells.**—In order to drive more energetic reactions, individual photocells must be coupled to obtain larger potentials. The reaction



has a  $\Delta G^\circ = 1.36$  eV ( $pH = 0$ ), and would not occur in a cell of the type TIA/S/TIC, since the maximum available

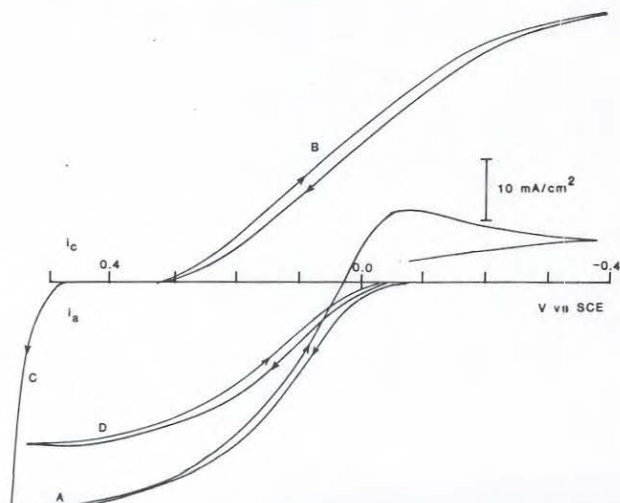


Fig. 11. *i*-*V* behavior in 48% HBr for a TIA (A), TIC (B), and Pt electrode (C). TIA response after addition of 1M phenol (D). Scan rate: 100 mV/s. Light intensity: 80 mW/cm<sup>2</sup>.

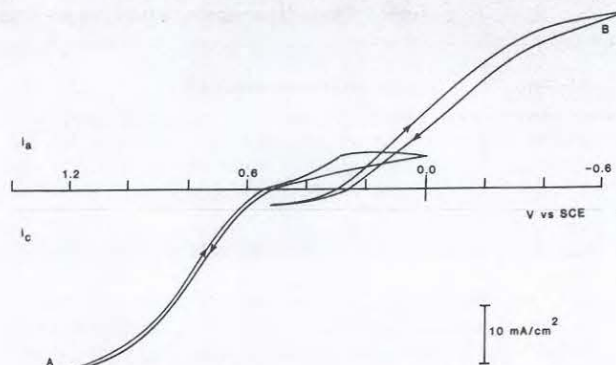


Fig. 12. *j*-*V* behavior for TIA (A) and TIC (B) in 5M HCl. Light intensity: 170 mW/cm<sup>2</sup>. Scan rate: 100 mV/s.

photovoltage is only ca. 1.1V. The coupling of two cells, TIA/S/TIC (cell 2) and TIA/S/TIC (cell 1), where cell 1 contains a single redox couple, which provides a bias to cell 2, will produce a photopotential large enough for HCl electrolysis to occur in cell 2. The *i*-*V* curves for both a TIA and a TIC in 5M HCl are given in Fig. 12. The overlap is poor, and coupling these electrodes resulted in no observable short-circuit photocurrent. However, addition of the bias from cell 2 (coupled as in Fig. 5) did result in a net short-circuit photocurrent. For the case of cell 1 containing 1.0M  $Br_2$ /1.0M KBr, the observed value of  $j_{sc}$  was 7.3 mA/cm<sup>2</sup> with  $V_{oc}$  being 2.0V with illumination intensity of 170 mW/cm<sup>2</sup>. Table II gives values of  $j_{sc}$  for various conditions in cells 1 and 2. As predicted from the *i*-*V* characteristics for individual half-cells (Table I), the  $Br^-/Br_2$  couple gave the best behavior. Moreover (see Table II), more acidic conditions favor the reaction, since the proton reduction reaction shifts towards more positive potentials with decreasing pH but the  $Cl^-$  oxidation is invariant with pH. Efficiencies for the coupled cell arrangement are also given in Table II. The efficiency,  $\phi$ , is defined as

$$\phi = P_e I \quad [7]$$

where  $P_e$  is the power stored as free energy in the electrolysis products and  $I$  is the incident light intensity.  $P_e$  was evaluated by assuming the products are consumed in a fuel cell reaction at the same current density as that for their production. Therefore, we take

$$P_e = j_{sc} \times E^\circ \quad [8]$$

where  $E^\circ$  is the standard potential for rereaction, -1.36V.

**Photoarrays in nonaqueous media.**—Halogenation in nonaqueous media is possible at the TIA, as demonstrated by the following results for the chlorination of cyclohexene in acetonitrile (MeCN) (19). The photo-oxidation of  $Cl^-$  at a TIA occurs with  $V_{onset}$  ca. 0.5V vs. SCE (Fig. 13). The cathodic wave indicates that some of

Table II. Photoelectrolysis of HCl with different coupling solutions

Cell conditions <sup>a</sup>		$j_{sc}$	$P_e$	$\phi$ (%)
Compartment A	Compartment B	(mA/cm <sup>2</sup> )	(mW/cm <sup>2</sup> ) <sup>b</sup>	
11.6M HCl	1.0M $Br_2$ 1.0M KBr	7.3	9.9	5.8
5.0M HCl	1.0M $Br_2$ 1.0M KBr	6.7	9.1	5.3
5.0M HCl	2.0M $FeCl_2$ 2.0M $FeCl_3$	3.3	5.4	3.2
1.0M HCl	1.0M HCl 2.0M $FeCl_2$ 2.0M $FeCl_3$ 1.0M HCl	2.7	3.7	2.2

<sup>a</sup> Cell configuration as in Fig. 5; illumination intensity 170 mW/cm<sup>2</sup>.

<sup>b</sup> Short-circuit conditions approximated with  $R_i = 15\Omega$ .

